www.cadanda.com
Computer-Aided Design AND APPLICATIONS

Shape Descriptor-Based Similar Feature Extraction for Finite Element Meshing

Hideyoshi Takashima[1] and Satoshi Kanai[2]

[1]Hokkaido University, hideyoshi_takashima@ais-hokkaido.co.jp
[2]Hokkaido University, kanai@ssi.ist.hokudai.ac.jp

Corresponding author: Satoshi Kanai, kanai@ssi.ist.hokudai.ac.jp

Abstract. The aim of this paper is to propose a feature extraction method that allows for the extraction of features that contain nonidentical geometries from a target shape, which are similar to that of a reference feature shape. In this method, the reference feature shape and target shape are represented by a set of shape descriptors defined in triangular meshes. The proposed similar feature extraction method was verified by some case studies in which the relationships between the reference shape and target shape were isotropic scaling, anisotropic scaling, and anisotropic scaling with distortion and complex deformation. In most cases, local regions having similarity to a reference feature could be successfully extracted from a target shape. The results show that the proposed shape descriptor-based feature extraction method effectively allows an engineer to identify where local regions, having similarity to a reference feature, are placed on a target shape. However, the estimated projective transformation in the method still includes non-negligible errors that are not good enough to fit the reference mesh model to the similar features extracted. This dilemma is seen as an appropriate avenue for future research.

Keywords: Feature Extraction, Shape Descriptor, Key Point Matching, SHOT, Shape Index, Projective Transformation, Triangular Mesh, Finite Element Method.
DOI: https://doi.org/10.14733/cadaps.2021.1080-1095

1 INTRODUCTION

Large-scale computer-aided engineering (CAE) has been significant in the ever-growing importance of its role as the digitalization of automotive manufacturing gains pace and as its development process becomes more streamlined. Finite element (FE) models that are used in large-scale CAE such as vehicle crash simulations, pedestrian impact simulations, noise vibration and harshness simulations, must be composed of high-quality FE meshes that comply with the in-house meshing specifications defined based on the design policies and past experiences of vehicle manufacturers. Moreover, not only the manufactures but also the third parties engaging in outsourcing FE analysis must respect the specifications when they create FE meshes in the FE-analysis.

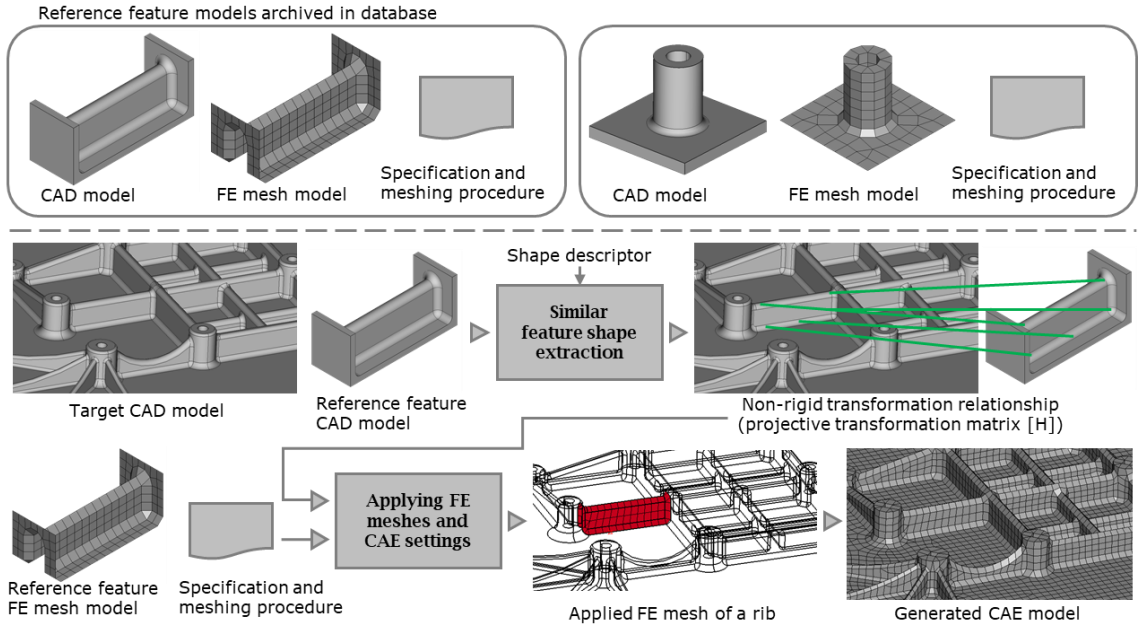

Figure 1: Non-rigid transformation relationship mapping-type CAE model generation system: The first step is similar feature shape extraction of features containing nonidentical geometries similar to a reference feature shape from a target shape. The second step is applying meshes and CAE settings such as rigid constraints, to extracted feature region.

In most of the FE meshing specifications, each specification is represented as a combination of a specific type of form features and the FE meshing pattern imposed on it. Typical examples are the following: (1) "when the FE mesh is created for a cylindrical boss feature, the node points of the elements must be placed concentrically around a medial axis of the boss at the specified regular angle intervals" or (2) "when the FE mesh is created for a rib feature, the nodes points must be arranged along a ridge curve on top of the rib at the specified regular length interval". These are required because a boss or rib is a lightweight substructure which generally has a significant role in maintaining the strength and stiffness of the whole product and the load paths going through the feature should be estimated as accurately as possible so as to guarantee the accuracy of FE analysis. If the elements in FE meshes are not arranged neatly in these features, the simulated load path differs considerably from the reality, and it eventually causes fatal design errors in the product. To avoid this situation, every manufacturer set their in-house meshing specifications that prescribe how fine and neatly the node points or elements in a FE mesh should be arranged and what kind of qualities the mesh should fulfil for a specific type of form features.

Of course, from the theoretical point of view in the analysis, the similarity of form features does not necessarily correspond to the similarity of physical behaviors estimated by FE analysis. However, from the communication point of view, the FE meshing patterns classified by the similarity of form features can offer a foolproof method to communicate the necessary conditions on FE meshing from the manufacturers to the outsourcers. By doing so, the engineers in the outsourcers can easily identify for which local regions in a product they should generate quality-assured FE meshes according to the specifications requested by the manufacturers.

Features prescribed in the meshing specifications are not confined to bosses and ribs. There are many other feature types that FE meshing patterns should be assigned for, such as holes, embosses, fillets, joggles, hemming, and gradually changing plate thickness. Therefore, more generally speaking, a "feature" in the meshing specification can be defined as a local region on the CAD model

of a product in which the analysis accuracy tends to be sensitive to its meshing quality and has already been known to be critical to the analysis reliability from the manufacturer's past experiences.

However, automatic feature-compliant mesh generation is not fully supported in the current commercial CAE software, thus requiring many manual operations, which resulting in high person-hour ratio in the whole CAE process. There are some reasons why this difficulty arises in the automatic feature-compliant mesh generation, which include the following:

- Even if the native format file of a CAD model explicitly includes the form feature information for the analysis, the information usually cannot be exported to the standard exchange file format, and only a boundary representation (B-rep) solid model that does not include any feature information can only be imported to the CAE preprocessor for mesh generation. Therefore, the feature extraction from the CAD model is still needed for the mesh generation.
- Unlike machining features [5], the features prescribed in the meshing specifications mainly consist of free-form surfaces, and their geometries are not uniquely shaped and are usually bounded by smooth and indistinct boundaries. Therefore, it is not so straightforward to design and implement procedure-oriented or rule-oriented feature extraction algorithms on the CAD model of a product.
- There is a great diversity in the geometries of features for FE meshing. Even ribs and bosses vary substantially in shapes and boundary geometries. Moreover, the features are not limited to bosses or ribs but have many variations, such as holes, embosses, fillets, and joggles, because the analysis accuracy tends to be sensitive to the meshing qualities on these regions and the definition of the features for FE meshing differs manufacturer by manufacturer. Therefore, it is difficult to realize a versatile feature extraction algorithm applicable to all feature types especially in procedure-oriented or rule-oriented approach. Consequently, different extraction algorithms or rules must be designed and implemented for different feature types.
- If the CAD model of a product includes product data quality (PDQ) problems, the models are would appear connected and watertight when they are practically disconnected and not watertight and have "holes" in the topological sense. In the mesh generation by CAE preprocessors, these defects eventually cause to generate poor-quality FE meshes, such as invisible holes, elements with infinitesimal sizes, and unacceptably distorted elements, or to fail the mesh generation at all. The elements with exceedingly small sizes force the solver to decrease the time step of the analysis and extremely increase the calculation time for keeping the stability of numerical calculation in case of dynamic analysis. Additionally, they make the simulation especially difficult to finish in realistic time. Moreover, the distorted elements also degrade the stability and accuracy of numerical calculation. In this way, the PDQ problems often cause difficulty to automatically generate FE meshes complying with the meshing specifications and analysis accuracy requirements. Similarly, the PDQ problems also cause difficulty for the feature extraction algorithm to automatically select the form features for FE meshing from the boundary faces of a CAD model by relying only on the topological connectivity among the faces. As a result, many manual efforts needed for fixing these poor-quality FE meshes involve substantial time and cost using CAE preprocessors.

Therefore, an automated feature extraction technique that targets feature-compliant FE meshing is strongly required wherein the features on a target shape whose geometries are not necessarily identical but rather similar to those of a reference feature shape can be extracted from the target CAD model of a product.

Researchers have proposed methods of extracting form features from a target CAD model to generate meshes of FE models [12][13][15]. However, in these studies, three main problems persist as follows:

- Feature extraction does not work robustly when a CAD model has PDQ issues, such as cracked or degenerated geometries, because extraction algorithms mainly rely on topological connectivity among the faces on a CAD model that is represented as a B-rep solid model.
- Features that are surrounded by complex and smooth fillet-like boundaries, which are commonly found in the features for FE meshing, such as bosses and ribs in cast or forged parts, remain difficult to detect because the algorithms assume that the features to be extracted are bound by sharp and distinct edges.
- A different extraction algorithm must be designed in an ad hoc way for different form feature types even if the features have similar shapes and the difference in shapes among them is little. Thus, it is difficult to reuse the previous methods for feature extraction from CAD models when developing feature-compliant FE meshing.

So, as a solution to these main problems, an automatic feature extraction method that is aimed at FE meshing and that allows for the extraction of form features, whose shape has similarity relationship with a reference feature shape, from a target shape that is expressed by a B-rep CAD model was proposed. Figure 1 illustrates how the proposed feature extraction method is utilized as part of the FE meshing process. A set of reference feature models that is composed of a solid CAD model, an FE mesh model that corresponds to the CAD model and FE meshing specifications is archived in a database. The FE meshing specifications include FE meshing patterns for feature and analysis conditions, such as rigid constraints, like bolt connections imposed on a feature surface. Then, the proposed similar feature extraction method is used to find feature regions, whose geometries are similar to those of the reference feature models on the surface of the target CAD model. Finally, the feature-compliant FE meshing method is applied to the extracted feature regions to generate a partial FE mesh of the feature that complies with FE meshing specifications, such as mesh resolution, node placement constraints, and analysis conditions. However, this paper only focuses on how feature regions that are similar to a reference feature shape are extracted from a target CAD model.

In the proposed method, the reference feature shape and target shape are represented by a set of shape descriptors defined in triangular meshes. Feature extraction is performed by first finding the correspondences between the descriptors of the reference feature shape and those of the target shape. Based on the correspondences, non-rigid transformation of the reference feature shape into the target shape is estimated and validated. If a valid non-rigid transformation is found, the corresponded feature regions on the target CAD model are outputted. Then, transformation is applied to the FE mesh model in the reference feature model where the reference FE mesh is deformed to fit with the shape of the extracted feature regions on the target CAD model. At the same time, the FE meshing specification linked to the reference feature model is automatically assigned to the deformed reference FE mesh.

The advantages of the proposed similar feature extraction method are summarized as follows:

- For feature extraction, solid models of a reference feature and a target shape are transformed into dense triangular meshes in advance. The shapes are represented by shape descriptors that are defined only at the dense vertices sampled on the meshes, and all we need for the feature extraction algorithm is the discrete point clouds independently sampled on triangles of the triangular meshes. Therefore, the extraction algorithm does not rely on any topological connectivity among the faces on the solid models. Consequently, even if the original solid model or triangular meshes have PDQ issues, such as cracked or degenerated geometries, the point sampling on each triangle can still work, and it only exerts little influence on the extraction process. It improves the stability of the feature recognition process for FE mesh generation.
- Sometime, the analysis engineer is asked to perform FE analysis from B-rep models generated by reverse engineering of the low-level three-dimensional (3D) scanned point clouds or triangular meshes measured from physical products. In this case, the B-rep models tend to include more nonuniform rational basis spline (NURBS) surfaces with

valuable PDQ problems, such as fine cracks between surfaces, than the case that the models originally generated by CAD systems. However, the proposed recognition algorithm only relies on the sampled points on the tessellated meshes. Also, the processing stability of the point sampling on the triangles does not degrade whether the model is created by CAD systems or reverse engineering and whatever the surface type is.

- The proposed extraction method is implemented based on the similarity-based part-in-whole matching principle. According to the principle, the similarity between a reference feature and part of a product model is evaluated only by the similarity in curvature-based local shape descriptors sampled discretely on both surfaces. So the evaluation is only dependent to the spatial distribution of curvatures inside the feature surface. It means that the extraction does not greatly depend on the feature boundary shapes, and the extraction algorithm can work regardless whether the feature is composed of complex free-form features or not or whether it is bounded by sharp or smooth boundary edges. Therefore, the scope of the features that can be extracted is extensive.
- A simple extraction algorithm needs to be implemented for any type of feature for FE meshing because the algorithm is based on the geometric similarities in descriptors between the reference feature and the target shape. Therefore, even if the types of features to be extracted are increased, we only have to change the reference feature shape and do not have to modify the extraction algorithm itself. Moreover, the algorithm can extract partial regions on a target shape not only identical to the reference feature but also similar to it. It means that the partial regions on the target shape that have a parametrically deformed relationship with the reference feature shape can be extracted. So, the compact set of the reference models only have to be archived in the database. As a result, the versatility of the feature recognition algorithm can be reinforced.

Of course, our feature recognition algorithm from low-level tessellated geometry may introduce a certain amount of complication in the algorithm compared to the conventional recognition algorithm directly from a B-rep solid model. But given the above-described reasons, it can greatly improve the stability and versatility of the feature recognition for FE mesh generation.

The latter part of the paper is organized as follows. In section 2, related works are reviewed and issues are clarified. In section 3, the details of the feature extraction algorithms are described. In section 4, the results of case studies are shown. Finally, in Section 5, the conclusion is presented.

2 RELATED WORK

This study is related to the research fields of form feature extraction in computer-aided design and computer-aided manufacturing (CAD/CAM), part-in-whole shape retrieval, and 3D object recognition. In this section, a related works in the field were reviewed, and the drawbacks will be discussed from the aspect of feature extraction for FE modeling.

2.1 Form Feature Extraction in CAD/CAM

So far, there has been considerable research on feature extraction techniques in traditional CAD and manufacturing area, which includes machining feature extraction from solid models that has been studied intensively since the 1990s. An overview of machining feature extraction techniques is well reviewed in [5]. However, the features that they deal with, such as slots and pockets, are bound by sharp and distinct edges. It could be difficult for these techniques to extract features that are surrounded by complex and smooth fillet-like boundaries, which are commonly found in bosses and ribs on cast or forged parts and are crucial features for FE meshing.

Unlike machining feature extraction techniques, there are only few studies on the feature extraction aimed at FE meshing thus far. However, lately, there have been increasing studies [3][12][13][15][22][24]. In most of them, ribs and bosses are extracted from a solid model of a target shape. Graph-based and rule-based approaches are used to derive features from a solid model

[3][12][15][22]. However, in both approaches, the extraction algorithms or rules are elaborated for specific feature types, and a new algorithm or rule must be designed if a new feature type to be extracted has to be added.

On the other hand, feature extraction and volume decomposition methods are developed to automatically generate feature-oriented FE meshes [13][24]. Rule-based approach is used to extract swept features and volumes from a solid model, whose shapes are suitable for automatic hexahedral FE meshing. However, extraction rules are specifically designed for a swept feature and hexahedral meshing and highly rely on topological loop patterns and local geometric relationship with a solid model. Therefore, the extraction algorithm lacks flexibility and does not work robustly if the CAD model has PDQ issues.

The recognition of geometric similarity between a reference feature shape and local regions of a target shape is another useful technique in automated FE meshing and modeling. Based on the concept, recently, a similar subpart search technique for FE meshing on a solid model has been proposed [15]. In the technique, subparts on the target shape that are similar to the archived subparts of proven FE models are extracted from a newly designed CAD model of the target shape. The similarity among the subparts is evaluated from topological graphs with face geometry attributes of both the solid models. However, the approach strongly relies on the topological graphs of a solid model and does not work robustly when a CAD model has PDQ issues. The approach might also fail if two subparts are geometrically similar to each other but have different topological structures because of non-uniqueness of the boundary representations of the object.

2.2 Part-in-Whole Shape Retrieval

Recently, there has been a great deal of research on 3D shape retrieval techniques, which is mainly in the field of computer graphics and 3D mesh processing. Detailed reviews are presented in [10] and [20]. Part-in-whole shape matching is among these techniques, which deals with essentially the same task as our feature extraction where local regions on a target shape that best matches a reference shape are found.

Part-in-whole matching among noisy triangular meshes is proposed in [9] wherein the local region of a target shape that best matches a reference shape is found. In their approach, feature point similarity and segment similarity are evaluated and integrated, and a probabilistic framework is introduced to enhance or moderate the certainty of feature point similarity. The method is effective in finding artifacts on a building that is congruent to a given artifact in the domain of archeology. However, it does not necessarily work if the region of a target shape to be found is not congruent to the artifact and has a parametrically deformed relationship with the reference shape. It is also not effective in the domain of FE modeling automation for industrial product design.

Attene et al. [2] proposed a part-in-whole matching schema called Fast Reject for efficient detection of local regions on a target 3D model that matches a reference shape, Furthermore, they implemented the scheme on the voxel-based raster representation of objects. The schema can extract the local region on a target shape that is sufficiently similar to the reference shape based on the similarity in shape descriptor. However, the degree of similarity could only be controlled by the threshold distance among the descriptors, and it is difficult to extract only the region on the target whose with the reference shape is parametrically deformed.

Hidaka et al. [7] developed a surface reconstruction system to create product models of civil structures from laser-scanned point clouds. Part-in-whole matching in point clouds was performed to find a set of representative parts that define major civil structures, such as bridge piers. However, this investigation is only focused on civil structure objects—so the target shapes could be represented by cuboids or cylinders—and is much simpler than the industrial products that we have to deal with in FE meshing.

Recently, some researchers have proposed a deep learning method for part segmentation of 3D point clouds wherein the point cloud of a whole shape is automatically partitioned into several semantic parts, as in [18] and [26]. Deep learning is a novel and attractive approach for feature

extraction, but so far, simple and distinct semantic parts can only be segmented, and the accuracy of segmentation still remains modest. Perpetrating the task of a large training set is also an issue from a practical aspect.

2.3 3D Object Recognition

In 3D computer vision and robotics, many 3D object recognition techniques wherein object instances of a given reference model were identified and extracted from a 3D measured point cloud have been developed. In recognition, key point matching with shape descriptors has a crucial role in finding object instances. Shape descriptor refers to a description method that utilizes a numeric descriptor called feature vector to characterize and encode a shape uniquely [10].

For example, Osada et al. [16] introduced the global shape descriptor, which is called shape distributions, of a whole object to content-based 3D shape retrieval wherein the histogram of distances between two randomly chosen points on a mesh surface yielded a robust shape descriptor. Furthermore, Ankerst et al. [1], Ip et al. [8] and Wohlkinger et al. [23] also proposed other histogram-based shape descriptors that are similar to that presented in [16]. However, these approaches are only aimed at evaluating the global similarity between two whole shapes using global descriptors and do not fit with the similar feature extraction problem we are dealing with.

On the other hand, for object recognition in robotics, Tombari et al. [21] proposed a shape descriptor called signature of histograms of orientations (SHOT). The descriptor represents local curvature distribution of a local shape in a key point as a histogram and encodes it using a high-dimensional vector and thus is rotationally and translationally invariant. The descriptor exhibits high performance in 3D object detection from a 3D measured point. Shape descriptors similar to SHOT have also been proposed and utilized in robotic object recognition [4][6]. However, the objective of descriptor-based object recognition is to find the local regions of a measured point cloud that exactly matches a reference shape and it is not necessarily aimed at finding regions similar to the reference shape like our objective.

The shape classification of free-form features for FE meshing based on point feature histogram (PFH) and thickness histogram descriptor is also proposed in [19], and complex free-form feature shapes represented by triangular mesh can be accurately classified into boss or rib features using two shape descriptors and a machine learning classification technique. However, a huge number of training samples are needed for classification. Moreover, they do not propose any method for extracting a feature shape from a target shape.

As part of shape descriptors, shape index (SI) is proposed as a local signature that represents local curvature distributions at a key point, but unlike [4][6][20], SI is scale-invariant [11]. Therefore, the local regions of a measured point cloud that have an isotropic scaling relationship with the reference shape can be detected. Itskovich et al. [9] proposed a part-in-whole detection method of archeological artifacts based on the similarity in SI descriptors at salient points. SI descriptors is also applied to medical science field. Techniques for the automatic detection of polyp candidates from computed tomography (CT) volume data are proposed based on the curvature analysis in [17][25]. In these techniques, SI is used for the classification of polyp shape candidates. However, the techniques in these references assume that the relation between the reference shape and local region shape in a whole object is limited to an isotropic scaling. Moreover, feature extraction techniques that only use SI do not work if the local regions of a measured point cloud have an anisotropic scaling relationship with a reference shape.

3 PROPOSED SIMILAR FEATURE EXTRACTION METHOD

3.1 Basic Concept

The proposed similar feature extraction method exhaustively finds local regions on a target shape represented by a solid model whose shape and size are similar to those of the reference feature shape prespecified by a user. The intended features include, but are not limited to, ribs and bosses

in cast or molded parts. This methodology aims to solve the three mainly identified issues via the approaches described in the succeeding text.

- Representations of the target shape and reference feature shape are converted from solid models into triangular meshes, which will be used for extracting similar features. This enables stable feature extraction even if a solid model has PDQ-degraded geometries and/or if the feature shape boundaries are ambiguous.
- Shape descriptors defined on a triangular mesh are applied in feature extraction. This approach has demonstrated to have aided in object recognition and similar shape retrieval in meshes and point clouds. Using this descriptor-based approach, an extraction algorithm can be unified even with different feature types or features with similar shapes.
- Local regions that have a projective transformation relationship with the reference feature can be extracted from a target shape. It allows for the extraction of feature shapes that have a parametric deformation relationship with the reference feature shape.

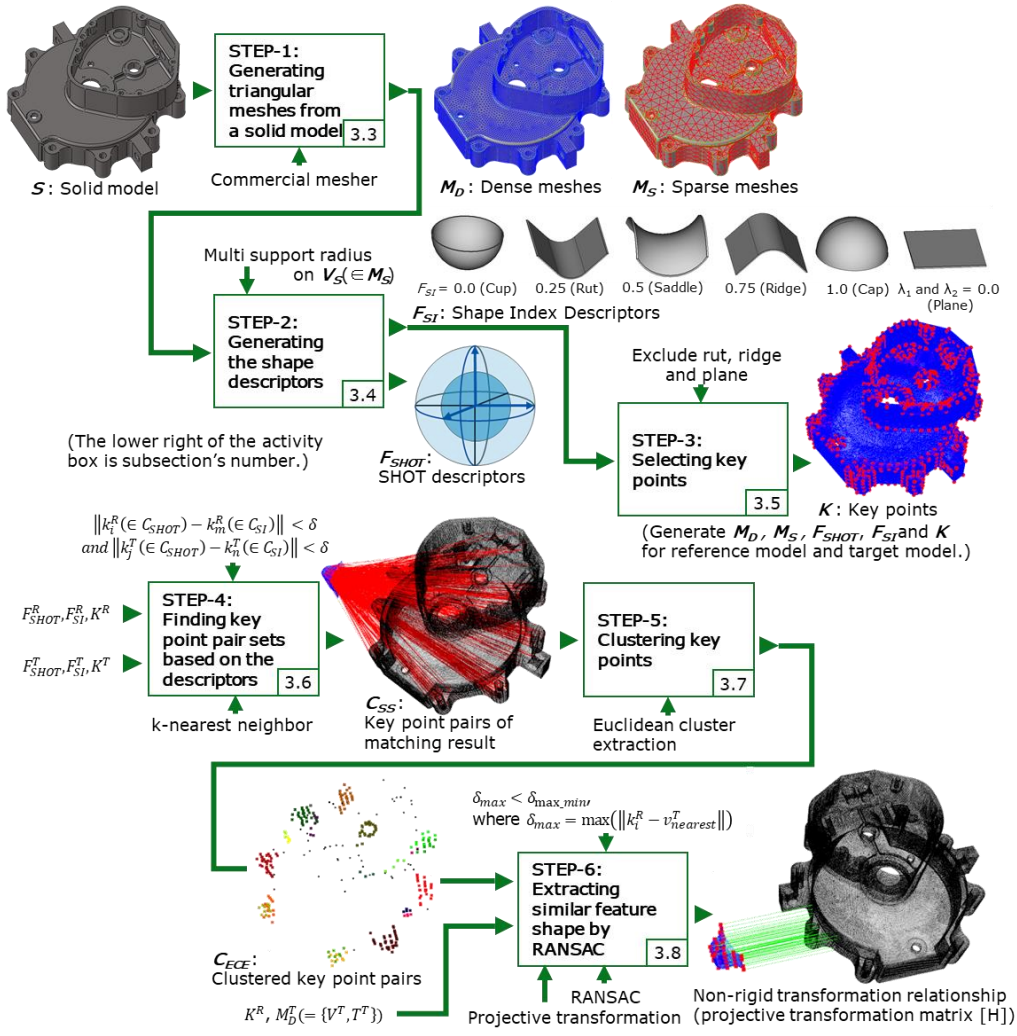

Figure 2: Procedure for proposed similar feature shape extraction. Steps 1–3 create shape descriptors of target and reference feature shapes. Steps 4–6 search for feature shapes similar to the reference shape.

3.2 Similar Feature Shape Extraction Procedure

The proposed similar feature extraction method is comprised of six steps and is summarized in Figure 2. Steps 1–3 create the shape descriptors of the target and reference feature shapes. Steps 4–6 search for feature shapes that are similar to the reference shape.

3.3 Step 1: Generating Triangular Meshes from Solid Model

Dense triangular mesh $M_D^T = \langle V_D^T, T_D^T \rangle$ (where V_D^T and T_D^T are vertex and triangle set, respectively) and sparse triangular mesh $M_S^T = \langle V_S^T, T_S^T \rangle$ are generated from one solid model S^T of the target shape using a CAE preprocessor. Similarly, triangular meshes $M_D^R = \langle V_D^R, T_D^R \rangle$ and $M_S^R = \langle V_S^R, T_S^R \rangle$ of the reference feature shape to be extracted are also generated.

Dense triangular meshes are necessary to calculate a feature shape descriptor with high accuracy. On the other hand, sparse triangular meshes are necessary to select a small number of distinctive feature key points with low calculation cost. It is not required that the vertices of the sparse mesh are the subset of those in the dense mesh and that the dense and sparse meshes are not conformal with each other, since the distinctive feature key points are used to estimate the transformation between a reference feature shape and a target shape, while the shape descriptors are used to validate the shape similarities between them. However, if the calculation cost is not significant, it is also possible to use the dense triangular meshes as a sparse triangular mesh.

3.4 Step 2: Generating Shape Descriptors

SI descriptor $f_{SI,i}^T$ [9][11][17][25] and SHOT descriptor $f_{SHOT,i}^T$ [21] are calculated at each vertex $v_{S,i}^T (\in V_S^T)$ of sparse triangular mesh M_S^T to create SI descriptor set $F_{SI}^T = \{f_{SI,i}^T\}$ and SHOT descriptor set $F_{SHOT}^T = \{f_{SHOT,i}^T\}$, respectively. To reduce the scale dependency of the SHOT descriptor, each descriptor $f_{SHOT,i}^T$ is evaluated at $v_{S,i}^T$ using multiple radii of the support sphere. Similarly, descriptor sets $F_{SI}^R = \{f_{SI,i}^R\}$ and $F_{SHOT}^R = \{f_{SHOT,i}^R\}$ of the reference feature shape to be extracted are created.

SI descriptor $f_{SI,i}$ expresses the degree of curvedness of the local surface around vertex v_i as a single scalar value and has scale and rotation-invariant property. SI descriptor $f_{SI,i}$ [9] is defined by the maximum and minimum principal curvatures λ_1 and λ_2 at v_i as Equation (3.1):

$$f_{SI,i} = \frac{1}{2} - \frac{1}{\pi} tan^{-1}\left(\frac{\lambda_1 + \lambda_2}{\lambda_1 - \lambda_2}\right). \tag{3.1}$$

In an exceptional case that the local shape is planar and λ_1=0.0 and λ_2=0.0, SI descriptor is not defined mathematically from Equation (3.1) but, in this case, we assign a special value to the descriptor to represent this planarity. As shown in Figure 2, by the value of $f_{SI,i}$, the curvedness of a local shape corresponds to the value of SI descriptor, for example, cup ($f_{SI,i} = 0.0$), rut ($f_{SI,i} = 0.25$), saddle ($f_{SI,i} = 0.5$), ridge ($f_{SI,i} = 0.75$) and cap ($f_{SI,i} = 1.0$). The SI descriptor value $f_{SI,i}$ is used for selecting the vertices with high distinct feature in Step 3.

On the other hand, the SHOT descriptor is a 352-dimensional vector that encodes statistical distribution in a normal direction at the local vertices around v_i and is rotationally invariant [21]. Since this descriptor has high shape representation capability, matching accuracy can be improved.

3.5 Step 3: Selecting Key Points

Key points are a subset of vertices on a triangular mesh where descriptor values for feature extraction are evaluated. The adoption of a small number of distinct feature key points has demonstrated to have increased object recognition and localization reliability and to have decreased processing time [14]. As such, when SI descriptor $f_{SI,i}^T$ at vertex $v_{S,i}^T (\in V_S^T)$ of the target shape exhibits a surface with low distinct feature, that is, plane, rut, and ridge, that vertex is not selected as key point. Only the remaining vertices $v_{S,i}^T$ are adopted as key point set $K^T = \{k_i^T\} (\subset V_S^T)$. The SI and SHOT

descriptors at key point $k_i^T(\in K^T)$ are adopted as feature descriptor sets $F_{SI(k)}^T = \{f_{SI(k),i}^T\}(\subset F_{SI}^T)$ and $F_{SHOT(k)}^T = \{f_{SHOT(k),i}^T\}(\subset F_{SHOT}^T)$, respectively. Similarly, key point set $K^R = \{k_i^R\}(\subset V_S^R)$ and feature descriptor sets $F_{SI(k)}^R = \{f_{SI(k),i}^R\}(\subset F_{SI}^R)$ and $F_{SHOT(k)}^R = \{f_{SHOT(k),i}^R\}(\subset F_{SHOT}^R)$ are generated for the reference feature shape.

3.6 Step 4: Finding Key Point Pair Sets Based on Descriptors

For each SHOT descriptor $f_{SHOT(k),i}^T(\in F_{SHOT(k)}^T)$ at key point $k_i^T(\in K^T)$ on the target shape, N corresponding key points are searched from key point set $K^R = \{k_j^R\}$ on the reference feature shape according to the ascending order of distance $\|f_{SHOT(k),j}^R - f_{SHOT(k),i}^T\|$, creating the nearest key point pair set with respect to SHOT $C_{SHOT} = \{(k_j^R, k_i^T)_p \mid p \in [1,N], k_i^T \in K^T\}$. Similarly, the nearest key point pair set with respect to SI $C_{SI} = \{(k_n^R, k_m^T)_q \mid q \in [1,M], k_m^T \in K^T\}$ is generated by evaluating distance $\|f_{SI(k),n}^R - f_{SI(k),m}^T\|$.

As the SI and SHOT descriptors express local curvatures in different forms, key point pairs that have higher similarity are then selected from C_{SHOT}. This is done by selecting key point pairs from C_{SHOT} with high correspondence between the SHOT and SI descriptors, which means that there is at least one nearest key point pair in C_{SI} close to a given nearest key point pair C_{SHOT} within distance threshold δ, that is, $\text{dist}(k_i^T, k_m^T) < \delta \wedge \text{dist}(k_j^R, k_n^R) < \delta, (k_j^R, k_i^T) \in C_{SHOT}, \exists (k_n^R, k_m^T) \in C_{SI}$. If key point pair (k_j^R, k_i^T) in C_{SHOT} satisfies this condition, it will be stored in the new nearest key point pair set $C_{SS} = \{(k_j^R, k_i^T)\}(\subset C_{SHOT})$.

3.7 Step 5: Clustering Key Points

Key points $k_i^T \in (K_{SS}^T = \{k_i^T \mid (k_j^R, k_i^T) \in C_{SS}\})$ of the target shape included in key point pair set C_{SS} may be distributed to the multiple regions on the target shape that are similar to the reference feature shape. Thus, to increase the searching efficiency of the random sample consensus (RANSAC) algorithm that will be employed in Step 6, Euclidean clustering is applied to the key points in K_{SS}^T. Additionally, close feature key point pair set $C_{ECE} = \cup\, C_{ECE,l}$ is generated to aggregate the key points that are close to each other into one cluster $C_{ECE,l}$. Since the stability of the calculation algorithm for the projective transformation matrix depends on the distribution of vertices, the coordinates of the vertices of each cluster are normalized so that the mean is 0.0 and the standard deviation is 1.0. Similarly, the reference feature shape is normalized.

3.8 Step 6: Extracting Similar Feature Shapes Using RANSAC Algorithm

First, five key point pairs $\{(k_i^{RC}, k_j^{TC}) \mid k_i^{RC} \in K^{RC}, k_j^{TC} \in K^{TC}\}$ from one key point cluster $C_{ECE,l}$ are randomly selected. Projective 4x4 transformation matrix $[H]$, which transforms selected key point pairs $k_i^{RC}(\in K^{RC})$ into $k_j^{TC}(\in K^{TC})$, is then estimated using Equations (3.2) and (3.3) via lower–upper decomposition.

$$\frac{1}{w}[H]\{Q^R\} - \{Q^T\} = \{0\}, \tag{3.2}$$

$$[A]^T\{H\} = \{B\}, \tag{3.3}$$

where $[H] = [h_{ij}]$ is a 4×4 matrix with $h_{44} = 1$; $\{Q^R\}$ and $\{Q^T\}$ are the 4×1 homogeneous coordinates of key points k_i^{RC} and k_j^{TC}; w is the fourth component of $[H]\{Q^R\}$, that is $\sum_{i=1}^{4} h_{4,i} q_i^R$; $\{H\}$ is the 15×1 column vector in which all components of matrix $[H]$ are arranged in a column vector; and $[A]$ and $\{B\}$ are the 15×15 matrix and 15×1 column vector calculated from the coordinates of k_i^{RC} and k_j^{TC}, respectively. Second, the obtained projective transformation matrix $[H]$ is transformed into an original coordinate system before normalization in Step 5 by Equation (3.4).

$$[H]_{org} = [D]^T[H] \tag{3.4}$$

where $[D]$ is the matrix that transformed from the normalized coordinate to the original coordinate, and $[H]_{org}$ is the projective transformation matrix in the original coordinate system. Third, the transformed key point set $\widetilde{K^R}$ is generated by applying transformation $[H]_{org}$ to all key points except for the selected five in K^{RC}. The distance between each transformed key point in $\widetilde{K^R}$ and the closest vertex of M_D^T is then evaluated, so that the estimated transformation $[H]_{org}$ could represent an appropriate one. For this judgment, we first search the nearest point of $\widetilde{k_i^R}(\in \widetilde{K^R})$ from V_D^T using the k-nearest neighbor (kNN) algorithm and calculate error $\|\widetilde{k_i^R} - v_{D,nearest}^T\|$. Next, if maximum error $\delta_{max} = \max(\|\widetilde{k_i^R} - v_{nearest}^T\|)_{\widetilde{k_i^R} \in \widetilde{K^R}}$ of $\widetilde{K^R}$ is less than threshold $\delta_{\max\_min}$, we will update $\delta_{\max\_min}$ and $[H]_{org\_min}$. If $\delta_{\max\_min}$ is not updated after specified iterations of the updates, the estimation of $[H]_{org\_min}$ concludes. Finally, $[H]_{org\_min}$ gives the best projective transformation matrix that transforms the reference feature shape into a similar feature shape portion on the target shape.

The processes can be summarized in the following algorithm:

(1) Select randomly five key point pairs $\{(k_i^{RC}, k_j^{TC})\}$ from one key point cluster $C_{ECE,l}$.

(2) Estimate a projective transformation matrix $[H]$ from $\{(k_i^{RC}, k_j^{TC})\}$ using Equations (3.2) and (3.3).

(3) Transform the transformation matrix $[H]$ to the one $[H]_{org}$ with respect to the original coordinate system.

(4) Transform all the key points except for the selected five in $K^{RC} = \{k_i^{RC}\}$ using $[H]_{org}$ to generate $\widetilde{K^R}$.

(5) Evaluate the maximum distance δ_{max} between each transformed key point in $\widetilde{K^R}$ and its closest vertex in the dense mesh M_D^T.

(6) If $\delta_{max} < \delta_{\max\_min}$, update as $\delta_{\max\_min} \leftarrow \delta_{max}$ and $[H]_{org\_min} \leftarrow [H]_{org}$ and return to (1). If $\delta_{\max\_min}$ is not updated after the specified iterations or the iteration reaches the upper bound of iterations, go to (7). Otherwise, return to (1).

(7) The output $[H]_{org\_min}$ gives the best projective transformation matrix that transforms the reference feature shape into a similar feature shape portion on the target shape.

4 VERIFICATION OF SIMILAR FEATURE EXTRACTION

4.1 Matching with Deformed Ribs with Simple Shapes

To verify the proposed method, feature matching was performed on deformed ribs with simple shapes. Three deformation variations are included: isotropic scaling, anisotropic scaling and anisotropic scaling with distortion.

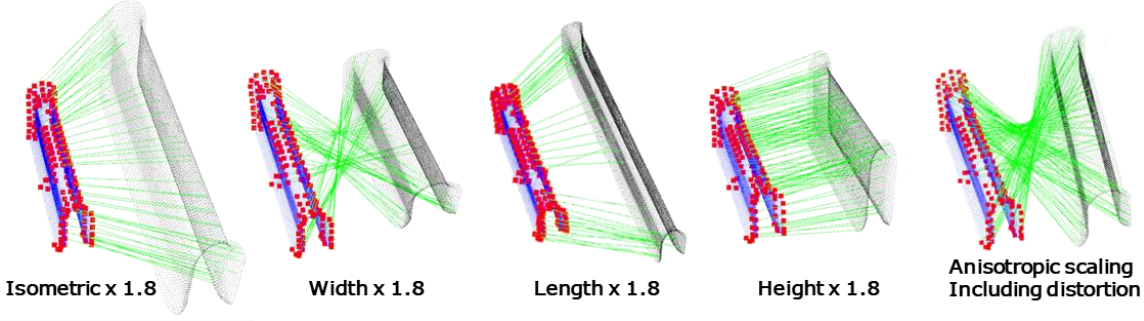

Figure 3: Matching results of deformed ribs

As a result, the deformed rib could successfully correspond with the reference rib, as shown in Figure 3. So far, the maximum feasible scale range was 1.8x in all cases. Because the rib of the reference feature shape was symmetrical, the matching lines sometimes intersected, as shown in Figure 3.

There is still room to expand the feasible scale range by optimizing the parameters and using a denser triangular mesh. However, in practice, even when the deformation ratio between the reference and target models exceeds 1.8, we can overcome this restriction of the scale range by preparing a few scaled versions of the original reference feature model beforehand.

4.2 Extraction of Similar Ribs and Bosses with Simple Shapes

Next, feature extraction was performed on a target flat-plate model that contains five similar ribs and bosses with simple shapes, as shown in Figure 4. In the five ribs and bosses, one was identical to the reference ribs and bosses, whereas the others were similar but had a top and bottom width different from the reference one. As the estimated projective transformation allowed for a high degree of freedom in deformation under original parameter settings, upon occasion, only a portion of the rib along the longitudinal direction was matched with the reference feature. To avoid a partial matching problem, the SI threshold was adjusted to allow the key points around the edge portions that exhibit strong geometric features to remain. Additionally, the upper and lower bounds of the volume expansion ratio, scale value and oblique distortion of projective transformation $[H]$ were defined. As a result, the five ribs were extracted correctly, as shown in Figure 5.

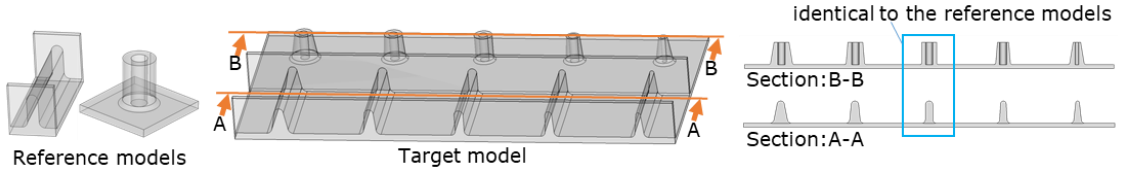

Figure 4: Test models of extraction of similar ribs and bosses with simple shapes

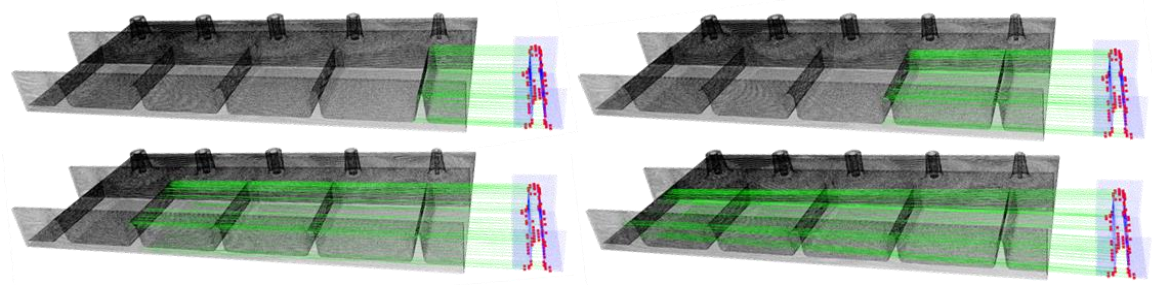

Figure 5: Extraction results of ribs with simple shapes

However, the bosses could not be extracted under the same settings because the local feature shapes are axially symmetrical in a circumferential direction. It increased the number of matching pairs that do not have projective transformation relationship with the boss shape. Consequently, it made the feature extraction by RANSAC difficult. This problem could have been avoided by limiting the intersection between matching pairs (intersection at each projection plane). However, there were actually few perfect axisymmetric shapes in the boss shape of industrial product parts. Therefore, this time, verification was performed by adding a small dummy shape in the circumferential direction of the boss to the reference shape and the target shape. As a result, four of the five bosses could be extracted successfully, as shown in Figure 6. However, one boss was not extracted to the last because the estimated deformation was too large. The aforementioned verification implies that adjusting the deformation threshold of $[H]$ to an appropriate range can make extraction possible.

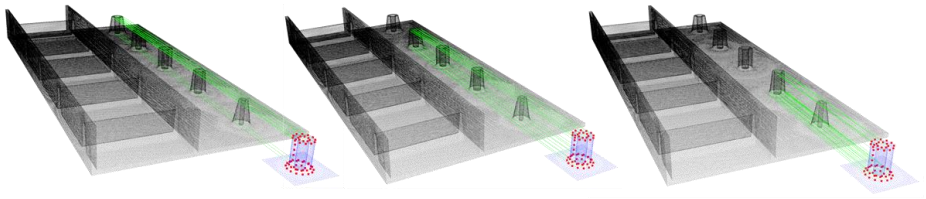

Figure 6: Extraction results of bosses with simple shapes.

4.3 Extraction of Complex Features with Anisotropic Scale

A second verification procedure was performed to determine if a feature shape whose anisotropic scale is different from that of the reference feature could be extracted. A target shape close to a cast product with various feature shapes, as shown in Figure 7, was selected. A portion of the target shape was cut out and deformed by anisotropic scaling to create the reference feature shape. The similar feature shape was successfully extracted, as shown in Figure 7. However, the feasible scale range differed in directions. Features of up to 1.5 times width and 1.2 times length were extracted. The limitation was specified by the bounds of the distortion constraint in projective transformation. Thus, expanding the anisotropic scale range would require extending the bounds of the constraints in projective transformation.

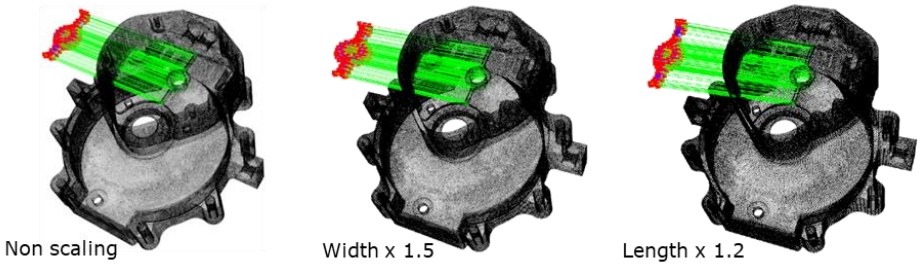

Figure 7: Extraction results of complex features with anisotropic scales (Red: key points of reference. Blue: reference. Black: target. Green: matching pairs.)

4.4 Extraction of Multiple Similar Features

A third extraction was performed to verify the extraction of multiple features with similar shapes on the same target shape, as shown in Figure 8. The reference feature shape was created by cutting out a local area in the target shape. Five of the six feature shapes were successfully extracted; the sixth could also be found by changing the mesh and the position of the reference feature. Thus, future work should aim to improve the robustness of extraction, possibly by increasing mesh density, equalizing sample density of key points between the reference feature and the target shape and finding the most suitable position of the reference feature shape for extraction.

Figure 8: Extraction results of multiple similar features. (Red: key points of reference. Blue: reference. Black: target. Green: matching pairs.)

4.5 Fitting FE Meshes with Extracted Similar Features

Finally, we tried to fit FE mesh models to the boss and rib features on the target shape that were extracted by the proposed method. The extracted projective transformation matrices were used for mesh fitting. The results are shown in Figure 9. As shown in the figure, the FE mesh model that was originally defined on the reference feature can be positioned approximately at the similar feature regions on the target shape. Therefore, the proposed method effectively allows an engineer to identify where local regions similar to a reference feature are placed on a target shape.

On the other hand, as also shown in the figure, the FE mesh model does not exactly fit the shape of the local regions that are similar to the reference feature on the target model since the estimated projective transformation in the method still includes non-negligible errors for fitting the reference mesh model to the similar features extracted. Therefore, completion of feature-compliant FE meshing remains an open issue and should be solved in our future work.

Figure 9: Results of applying extracted FE meshes: (a) applying FE meshes using extracted similar ribs and bosses with simple shapes and (b) applying FE meshes using extracted complex features with anisotropic scale and multiple similar features.

5 CONCLUSIONS

In this paper, we proposed a similar feature extraction to create an automatic feature-compliant FE meshing method focused in FE meshing that allows for extraction of form features, which have a shape similarity relationship with a reference feature shape, from a target shape. The method was based on a shape descriptor representation defined by a triangular mesh, matching operation between the reference feature shape and the target shape using descriptors and an estimation of projective transformation between them.

The proposed similar feature extraction method was validated by some case studies wherein the relationships between the reference shape and the target shape were isotropic scaling, anisotropic scaling, and anisotropic scaling with distortion and complex deformation. In most cases, local regions that are similar to a reference feature could be successfully extracted from a target shape. The results show that the proposed shape descriptor-based feature extraction method effectively allows an engineer to identify where local regions similar to a reference feature are placed on a target shape. However, the estimated projective transformation in the method still includes non-negligible errors that are not good enough to fit the reference mesh model to the similar features extracted.

In future works, we will attempt to solve the remaining issues, such as feature extraction technique for a boss with an axially symmetrical shape or a rib with the same cross section to longitudinal direction, to improve extraction accuracy. Furthermore, we will also focus in developing a method to assign appropriate FE meshing operations to extracted features in compliance with specifications. To do so, increasing the estimation accuracy of a projective transformation matrix that maps a reference feature to local regions on the target shapes by optimization is necessary. If the curvature of any point on the surface without topological connectivity of the solid model is obtained easily, it has the potential to obtain simpler, faster, and more accurate local descriptor calculation than the one proposed herein. This improvement remains as our future work.

Hideyoshi Takashima, https://orcid.org/0000-0002-7158-6059
Satoshi Kanai, https://orcid.org/0000-0003-3570-1782

REFERENCES

[1] Ankerst, M.; Kastenmler, G.; Kriegel, HP.; Seidl T.:3D shape histograms for similarity search and classification in spatial databases, Lecture Notes in Computer Science, 1651, 1999, 207-226. https://doi.org/10.1007/3-540-48482-5_14
[2] Attene, M.; Marini, S.; Spagnuolo, M.; Falcidieno, B.: The Fast Reject Schema for Part-in-Whole 3D Shape Matching, Eurographics Workshop on 3D Object Retrieval, 2010, 23-30. http://dx.doi.org/10.2312/3DOR/3DOR10/023-030
[3] Boussuge, F.; Leon, J.-C.; Hahmann, S.; Fine, L.: Idealized models for FEA derived from generative modeling processes based on extrusion primitives, Engineering with Computers, 31(3), 2015, 513-527. http://doi.org/10.1007/s00366-014-0382-x
[4] Drost, B.; Ulrich, M.; Navab, N.; Ilic, S.: Model globally, match locally: Efficient and robust 3d object recognition, 2010 IEEE Conference on Computer Vision and Pattern Recognition, 2010, 998-1005. https://doi.org/10.1109/CVPR.2010.5540108
[5] Han, J.; Pratt, M.; Regli, W.C.: Manufacturing feature recognition from solid models: a status report, IEEE Transactions on Robotics and Automation, 16(6), 2000, 782-796. https://doi.org/10.1109/70.897789
[6] Hansch, R.; Weber, T.; Hellwich, O.: Comparizon of 3D interest point detectors and descriptors for point cloud fusion, ISPRS Annals of the Photogrammetry, Remote Sensing and Spatial Information Sciences, 2(3), 2014, 57-64. https://doi.org/10.5194/isprsannals-II-3-57-2014
[7] Hidaka, N.; Michikawa, T.; Yabuki, N.; Fukuda, T.; Motamedi, A.: Creating product models from point cloud of civil structures based on geometric similarity, The International Archives of Photogrammetry, Remote Sensing and Spatial Information Sciences, 40(4), 2015, 137-141. https://doi.org/10.5194/isprsarchives-XL-4-W5-137-2015
[8] Ip, C.Y.; Lapadat, D.; Sieger, L.; Regli, W.C.: Using shape distributions to compare solid models, Proceedings of the 7th ACM Symposium on Solid Modeling and Applications (SMA '02), 2002, 273-280. https://doi.org/10.1145/566282.566322
[9] Itskovich, A.; Tal, A.: Surface partial matching and application to archaeology, Computers & Graphics, 35(2), 2010, 334-341. https://doi.org/10.1016/j.cag.2010.11.010
[10] Iyer, N.; Jayanti, S.; Lou, K.; Kalyanaraman, Y.; Ramani, K.: Three-dimensional shape searching: state-of-the-art review and future trends, Computer-Aided Design, 37(5), 2005, 509-530. https://doi.org/10.1016/j.cad.2004.07.002
[11] Koenderink, J.J.; Doorn, A.J.: Surface shape and curvature scales, Image and Vision Computing, 10(8), 1992, 557-564. https://doi.org/10.1016/0262-8856(92)90076-F
[12] Lai, J.-Y.; Wang, M.-H.; Song, P.-P.; Hsu, C.-H.; Tsai, Y.-C.: Recognition and Decomposition of Rib Features in Thin-shell Plastic Parts for Finite Element Analysis, Computer-Aided Design and Applications, 15(2), 2018, 264-279. https://doi.org/10.1080/16864360.2017.1375678
[13] Lu, Y.; Gadh, R.; Tautges, T.J.: Feature based hex meshing methodology: feature recognition and volume decomposition, Computer-Aided Design, 33(3), 2001, 221-232. https://doi.org/10.1016/S0010-4485(00)00122-6
[14] Nagase, M.; Akizuki, S.; Hashimoto, M.: Reliable object recognition using 3-D feature points for minimizing its mismatching, Journal of The Japan Society for Precision Engineering, 79(11), 2013, 1058-1062. https://doi.org/10.2493/jjspe.79.1058
[15] Onodera, M.; Hariya, M.; Kongo, C.; Shintani, M.; Ka, K.; Watanuki, K.: Development of high precise similar sub-part search technique for automatic mesh generation reusing proven models, Transactions of The Japan Society of Mechanical Engineers, 85(880), 2019, 19-138. https://doi.org/10.1299/transjsme.19-00138
[16] Osada, R.; Funkhouser, T.; Chazelle, B.; Dobkin, D.: Shape distributions, ACM Trans. Graph, 21(4), 2002, 807-832. https://doi.org/10.1145/571647.571648

[17] Poo, M.; Buysee, E.; Carmona, R.; Coto, E.; Navarro, H.: GPU-accelerated Polyp Detection in Virtual Colonoscopy, CLEI electronic journal, 16(2), 2013, 3-3. ISSN 0717-5000
[18] Su, H.; Jampani, V.; Sun, D.; Maji, S.; Kalogerakis, E.; Yang, M. H.; Kautz, J.: SPLATNet: Sparse Lattice Networks for Point Cloud Processing, Proceedings of the IEEE Computer Society Conference on Computer Vision and Pattern Recognition, 2018, 2530-2539. https://doi.org/10.1109/CVPR.2018.00268
[19] Takaishi, I.; Kanai, S.; Date, H.; Takashima, H.: Free-Form feature classification for finite element meshing based on shape descriptors and machine learning, Proceedings of CAD'19, 2019, 414-419. https://doi.org/10.14733/cadconfP.2019.414-419
[20] Tangelder, J.W.H.; Veltkamp, R.C.: A survey of content based 3D shape retrieval methods, Multimedia Tools Applications, 39, 2008, 441-471. https://doi.org/10.1007/s11042-007-0181-0
[21] Tombari, F.; Salti, S.; Stefano, L.D.: Unique Signatures of Histograms for Local Surface Description, Proceedings of the European Conference on Computer Vision 2010, Part 3, 2010, 356-369. https://doi.org/10.1007/978-3-642-15558-1_26
[22] Wang, M.-S.; Lai, J.-Y.; Hsu, C.-H.; Tsai, Y.-C.; Huang, C.-Y.: Boss Recognition Algorithm and Application to Finite Element Analysis, Computer-Aided Design and Applications, 14(4), 2017, 450-463. http://doi.org/10.1080/16864360.2016.1257187
[23] Wohlkinger, W.; Vincze, M.: Ensemble of shape functions for 3D object classification, Proceedings of the IEEE International Conference on Robotics and Biomimetics, 2011, 2987-2992. https://doi.org/10.1109/ROBIO.2011.6181760
[24] Wu, H.; Gao, S.: Automatic swept volume decomposition based on sweep directions extraction for hexahedral meshing, Procedia Engineering, 82, 2014, 136-148. https://doi.org/10.1016/j.proeng.2014.10.379
[25] Yoshida, H.; Nappi, J.: Three-dimensional computer-aided diagnosis scheme for detection of colonic polyps, IEEE Transactions on Medical Imaging, 20(12), 2001, 1261-1274. https://doi.org/10.1109/42.974921
[26] Yuan, W.; Khot, T.; Held, D.; Mertz, C.; Hebert, M.: PCN: Point Completion Network,2018 International Conference on 3D Vision, Verona, 2018, 728-737. https://doi.org/10.1109/3DV.2018.00088